One-Terminal Traveling Wave-Based Transmission Line Protection for LCC-HVDC Systems

Rafael L. S. França, Francisco C. Silva Júnior, Flavio B. Costa, K. Strunz, and Athula D. Rajapakse

***Abstract*—This paper proposes a one-terminal traveling wave (TW)-based transmission line protection for line commutated converter (LCC) of high-voltage direct current (HVDC) systems. The method requires the first and second wavefronts to reach the local bus and considers the boundary conditions of the system. A detailed mathematical analysis of the sampling frequency effects, as the basis for a number of innovations of practical interest, is presented here. Firstly, a definition of a minimum sampling frequency is formulated. This is crucial when dealing with the high sampling frequencies traditionally needed by TW-based methods. Secondly, mathematical expressions of protected, unprotected, and uncertainty zones on the transmission line are defined. Thanks to these calculations, the method is also capable of distinguishing faults at the line terminals from faults on the protected transmission line. Thirdly, the non-requirement for the TW propagation speed estimation is proven. Some TW-based protection elements require knowledge of the TW propagation speed, which is a source of errors. The proposed function presented good dependability and was able to operate below 15 ms for a transmission line of 2900 km in length.**

***Keywords*—Boundary protection, LCC-HVDC transmission line protection, one-terminal protection, traveling waves.**

I. Introduction

The LCC-based HVDC technology is currently more economical than the HVAC option for bulk power transmission over distances above several hundreds of kilometers. A long overhead DC transmission line is exposed to hostile and unpredictable environmental conditions and often contributes to outages. In an HVDC system, the transmission line is the element that presents the highest failure rate [1]. Therefore, a fast and reliable protection system is essential to ensure safe operation and avoid damage to its assets.

The current change rate ($\mathrm{d}i/\mathrm{d}t$) based direction criterion associated with the current variation (Δ_i) based direction criterion is traditionally applied to the protection of HVDC transmission lines [2]. The effectiveness of the $\mathrm{d}i/\mathrm{d}t$ technique relies on the correct detection of the $\mathrm{d}i/\mathrm{d}t$ polarity to distinguish between forward and backward faults. Similarly, the Δ_i technique can detect the fault directionality according to the signal of the current variation. However, these functions are directional elements and present selectivity limitations [2].

The TW-based transmission line protection is divided, in general, into two- and one-terminal methods. The two-terminal ones require both a communication channel between the line terminals, which increases the protection operation time and, usually, a data synchronization scheme. This raises the cost of the protection scheme and makes the scheme reliability dependent on communication and synchronization systems. One-terminal methods require neither a communication channel nor data synchronization between the line terminals, resulting in lower costs and faster protection operations.

In [3], a one-terminal differential protection method is proposed. Nevertheless, many optical sensors are required, which increases the protection scheme cost. In [4] and [5], protection methods based on the transient energy and the transmission line terminal characteristics are proposed, respectively. However, both are two-terminal methods. One-terminal methods dependent on local measurement of transients have been proposed. In [6], a one-terminal protection method based on current transient harmonics and transmission line terminal characteristics is proposed. In [7], a one-terminal protection method based on transmission line terminal characteristics is proposed.

One-terminal TW-based protection methods have been proposed in [1], [8], [9], [10], [11]. However, usually, TW-based protection methods require higher sampling frequencies than those used in actual HVDC systems, which are a few tens of kHz. Therefore, protection functions that require higher sampling frequencies would hardly be implemented in actual HVDC systems. In addition, some TW-based methods require the TW propagation speed estimation, which is an error source. Close-in faults are usually issues for one-terminal TW methods based on wavefront arrival time detection. A definition of protection zones would contribute to protection selectivity and coordination.

Traditionally, the distinction between faults on the transmission line from faults on the line terminals is performed by two-terminal methods. This distinction is beneficial since it can speed up the location of the fault for maintenance purposes. In addition, for flexible bipole HVDC systems, the correct detection of a pole-to-ground fault on the transmission line allows reconfiguration to monopolar operation. Therefore, in case of faulty telecommunication, a one-terminal method that can provide selectivity for such fault cases is relevant.

The non-selective converter overcurrent protection is the fastest to trip actual HVDC systems. Moreover, AC breakers are traditionally used to clear faults in HVDC systems. Therefore, a fast selective operation time is beneficial, but an operation time below the opening time of the AC breaker is sufficient. This is typically from one-and-a-half to three cycles [12], i.e., for a 50 Hz power system, from 30 to 60 ms.

Only a few papers have investigated the effects of the sampling frequency process on TW-based protection and fault location to establish zones for protection [13] and fault location [14], respectively. Although fast and accurate, the approaches in [13], [14] are limited to

This study was financed in part by the Coordenação de Aperfeiçoamento de Pessoal de Nível Superior - Brasil (CAPES) - Finance Code 001, and by the Conselho Nacional de Desenvolvimento Científico e Tecnológico - Brasil (CNPq). R. L. S. França and F. C. Silva Júnior are with the Federal University of Rio Grande do Norte (UFRN), Natal, Brazil. F. B. Costa is with the Michigan Technological University, Houghton, USA. K. Strunz is with the Technical University of Berlin (TUB), Berlin, Germany. A. D. Rajapakse is with the University of Manitoba, Winnipeg, Canada.

Paper submitted to the International Conference on Power Systems Transients (IPST2023) in Thessaloniki, Greece, June 12-15, 2023.

two-terminal TW methods in AC systems. To avoid concerns with communication and data synchronization between line terminals, [15] considered the effects of the sampling frequency to propose a one-terminal method. However, [15] developed a traveling wave-based method strictly applied to earth faults and did not define the protection zones based on traveling wave arrival times. Therefore, to the best of the author's knowledge, the protection zones in one-terminal TW protection as a function of the sampling frequency have not been defined, and close-in faults are still a concern.

Continuing the methodology proposed in [13], [15] this paper contributes to the one-terminal TW protection of DC overhead lines in LCC-HVDC systems considering the effects of the sampling frequency in the local TW wavefronts. The proposed development considers boundary characteristics and the arrival times of the two first wavefronts to reach the local bus. Thus, information about TW magnitude and polarity is not required. The conventional one-terminal TW protection indicates whether a fault is internal or external considering the entire protected line as the protected zone. However, it presents errors for close-in line faults, which are detected as external faults. Conversely, as a novelty, the proposed one-terminal TW protection scheme considers the effects of the sampling rate to demonstrate the existence of protected, unprotected, and uncertain zones. Therefore, the zones where close-in faults are detected as external faults are predicted, which is important for protection selectivity and coordination.

As an additional contribution, an expression for evaluating the minimum sampling frequency that ensures proper DC line protection is introduced, which also has never been discussed in previous works. This expression demonstrates that high sampling rates in the order of MHZ are not mandatory in long LCC-HVDC lines and that the method can be implemented with a sampling frequency in the order of a few kHz with a reasonable protection zone. This equation indicates that short lines must only consider high-sampling frequency in the order of MHz. Some TW-based protection elements require knowledge of the TW propagation speed, which requires additional work and is a source of errors. However, as another contribution, this paper demonstrates that the speed of light can be adopted with no misoperation, yielding a protection system independent of the TW propagation speed estimation.

II. The Proposed Method

This paper considers the following definitions: 1) DC line boundaries: the series DC smoothing reactors, named here as series DC reactors, shunt DC filters, and DC buses; 2) AC line boundaries: transformers and AC filters; 3) AC faults: occur on AC systems, e.g., AC transmission lines or AC line boundaries; 4) DC external faults: take place at the converters or DC line boundaries; 5) close-in DC line faults: occur on the DC line but close enough to the DC line end on the unprotected zone, mathematically defined in this paper. This limitation is imposed in one-terminal TW methods by the sampling frequency as fully addressed in this paper; 6) DC internal faults: take place on the DC line with the exception of close-in DC line faults.

Both AC and DC line boundaries work as low-pass filters for TWs. Therefore, when AC and converter faults take place, high-frequency TWs are expected to be filtered out and do not sensitize TW-based protection systems on DC lines. Conversely, external DC and close-in DC faults may generate TWs that TW-based protection devices may detect as external faults. This paper proves mathematically that a well-defined protected zone can protect the DC line only in DC internal faults as expected. The traveling waves of all other faults, such as those from external DC, close-in DC faults, and AC faults (if they could cross the AC and DC filters), are detected as external events by detecting the first and second TW arrival times in just one terminal of the DC line.

A. General Idea of the Proposed Protection Scheme

Fig. 1 depicts the general idea of the proposed method. The protected DC transmission line has a length of d km and a fault at a distance d_{F} from the relay i positioned in the local station i is considered. From the fault inception time (t_{F}), TWs propagate from the fault point in both line directions. Thereafter, reflection or transmission phenomena occur whenever TWs encounter line terminals and the fault point. The proposed protection considers only aerial-mode traveling waves, obtained with the Karembauer transform.

The relay on the line terminal samples currents and voltages at a fixed time interval of $1/f_{\mathrm{s}}$, where f_{s} is the relay sampling frequency. A TW detection method detects wavefront arrival times by means of digital filtering-based methods, such as the wavelet transform [16], DS (differentiator-smoother) filter [17], or any other suitable method. The TW detection method provides the TW arrival times for the proposed method. However, even assuming no error in the TW detection, the sampling process itself results in errors in the identification of correct wavefront arrival times, which may affect the protection. For instance, the fault inception time is t_{F} in Fig. 1(b), whereas the wavefront arrival times at the local bus, which are referred to as the first and second TW arrival times are t_{F1} and t_{F2}, respectively. t_{F1} and t_{F2} refer to the continuous-time domain, and the relay is not capable of measuring them due to limitations imposed by the sampling process. Therefore, the arrival times in the discrete-time domain are $k_{\mathrm{F1}}/f_{\mathrm{s}}$ and $k_{\mathrm{F2}}/f_{\mathrm{s}}$ instead of t_{F1} and t_{F2}, respectively, where k_{F1} and k_{F2} are relay samplings sensitized by the first and second TWs, respectively. In addition, the

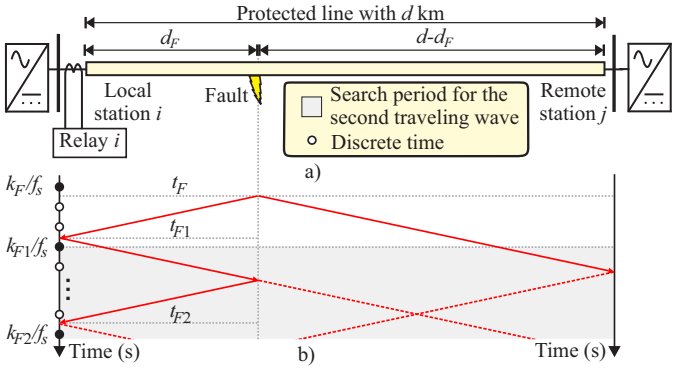

Fig. 1. General idea of the one-terminal TW-based transmission line protection: a) protected line; b) lattice diagram for an internal DC fault.

fault inception time is taken as $k_{\mathrm{F}}/f_{\mathrm{s}}$ instead of t_{F}, where k_{F} is the relay sampling related to the fault inception time. As a consequence, the error associated with the sampling process must be taken into account, as fully addressed in this paper.

B. Protection in the Discrete-Time Domain

Considering the sampling process, the arrival times t_{F1} and t_{F2} and the fault inception time t_{F} must be converted to the respective discrete times $k_{\mathrm{F1}}/f_{\mathrm{s}}$, $k_{\mathrm{F2}}/f_{\mathrm{s}}$, and $k_{\mathrm{F}}/f_{\mathrm{s}}$, respectively, as Fig. 1 depicts.

Based on Fig. 1, the error ϵ_{F} associated with the fault inception time and the errors ϵ_{F1} and ϵ_{F2} associated with the arrival times of the first and second wavefronts, respectively, are given by:

$$\epsilon_{\mathrm{F}} = t_{\mathrm{F}} - k_{\mathrm{F}}/f_{\mathrm{s}}, \tag{1}$$

$$\epsilon_{\mathrm{F1}} = k_{\mathrm{F1}}/f_{\mathrm{s}} - t_{\mathrm{F1}}, \tag{2}$$

and

$$\epsilon_{\mathrm{F2}} = k_{\mathrm{F2}}/f_{\mathrm{s}} - t_{\mathrm{F2}}, \tag{3}$$

where $0 \leq \epsilon_{\mathrm{F}} < 1/f_{\mathrm{s}}$, $0 < \epsilon_{\mathrm{F1}} \leq 1/f_{\mathrm{s}}$, and $0 < \epsilon_{\mathrm{F2}} \leq 1/f_{\mathrm{s}}$.

The difference between the discrete arrival times of the second and the first wavefronts, according to (2) and (3), is given by:

$$k_{\mathrm{F2}}/f_{\mathrm{s}} - k_{\mathrm{F1}}/f_{\mathrm{s}} = (t_{\mathrm{F2}} - t_{\mathrm{F1}}) + \epsilon_T, \tag{4}$$

where ϵ_T is the total error associated with the sampling rate, which takes into account the individual error of the wavefront discrete arrival time of the first and the second TWs. Since $0 < \epsilon_{\mathrm{F1}} \leq 1/f_{\mathrm{s}}$ and $0 < \epsilon_{\mathrm{F2}} \leq 1/f_{\mathrm{s}}$, then $-1/f_{\mathrm{s}} < \epsilon_T < 1/f_{\mathrm{s}}$.

According to the fault position on the protected line, the second wavefront to reach the local bus may originate from a reflection in the fault point or in the remote line end. The highest difference $t_{\mathrm{F2}} - t_{\mathrm{F1}}$ for an internal fault occurs for faults in the middle of the line, and it is equal to one transit time, d/v. Thus, from (4), an internal fault is detected when:

$$t_{\mathrm{F2}} - t_{\mathrm{F1}} \leq d/v \therefore k_{\mathrm{F2}} - k_{\mathrm{F1}} \leq (d/v + \epsilon_T)\, f_{\mathrm{s}}. \tag{5}$$

Considering the upper limit of the total error, (5) becomes:

$$k_{\mathrm{F2}} - k_{\mathrm{F1}} < (df_{\mathrm{s}}/v + 1)\,. \tag{6}$$

Since $k_{\mathrm{F2}} \geq k_{\mathrm{F1}}$, $k_{\mathrm{F1}} \in \mathbb{N}$, and $k_{\mathrm{F2}} \in \mathbb{N}$, from (6), when an internal fault occurs, the following expression is always true:

$$k_{\mathrm{F2}} - k_{\mathrm{F1}} \leq \lfloor df_{\mathrm{s}}/v \rfloor + 1. \tag{7}$$

When a fault takes place at the remote DC boundary, which is a DC external fault, the first TW will reach the local bus after a transit time d/v from the fault inception time t_{F}. Afterwards, it will be reflected toward the remote bus. When it reaches the remote bus, after a transit time, the TW suffers a new reflection and returns toward the local bus, lasting a transit time to reach it. Therefore, from (4) and due to a DC external fault we have:

$$t_{\mathrm{F2}} - t_{\mathrm{F1}} = 2d/v \therefore k_{\mathrm{F2}} - k_{\mathrm{F1}} = (2d/v + \epsilon_T)\, f_{\mathrm{s}}. \tag{8}$$

For faults in the local DC boundary, (8) is also true.

Considering the upper and lower limits of the total error, it follows from (8) that a DC external fault is detected if:

$$(2df_{\mathrm{s}}/v - 1) < k_{\mathrm{F2}} - k_{\mathrm{F1}} < (2df_{\mathrm{s}}/v + 1)\,. \tag{9}$$

Since $k_{\mathrm{F2}} \geq k_{\mathrm{F1}}$, $k_{\mathrm{F1}} \in \mathbb{N}$, and $k_{\mathrm{F2}} \in \mathbb{N}$, (9) becomes:

$$\lfloor 2df_{\mathrm{s}}/v \rfloor \leq k_{\mathrm{F2}} - k_{\mathrm{F1}} \leq \lfloor 2df_{\mathrm{s}}/v \rfloor + 1, \tag{10}$$

i.e., (10) is true whenever a DC external fault occurs.

Based on (7) and (10), the threshold to differentiate an internal from an external fault is given by:

$$k_{\mathrm{F2}} - k_{\mathrm{F1}} < \lfloor z \rfloor, \tag{11}$$

where z is given by:

$$z = pdf_{\mathrm{s}}/v, \tag{12}$$

and $\lfloor z \rfloor$ is a threshold which must satisfy:

$$\lfloor df_{\mathrm{s}}/v \rfloor + 1 < \lfloor z \rfloor \leq \lfloor 2df_{\mathrm{s}}/v \rfloor\,, \tag{13}$$

where p is a number that satisfies (13) and is further discussed in the following sections.

C. Close-in DC Line Faults

Fig. 2 depicts close-in DC line faults in order to highlight three situations as addressed in the remainder of this subsection. Fig. 2(a) shows a fault case situation where the two first wavefronts reach the local bus within the same sampling period, yielding to $t_{\mathrm{F2}} - t_{\mathrm{F1}} < 1/f_{\mathrm{s}}$. Thus, both wavefronts are detectable in the sample k_{F1} and their distinction would not be possible. However, the reflections and transmissions would occur quickly and the next samples would be sensitized with TWs. Therefore, a detection method could incorrectly indicate that the two first wavefronts have arrived in two following samples, i.e., in k_{F1} and k_{F1}+1. The proposed method overcomes this limitation by defining an unprotected zone to cover this situation, which will be further explained.

Fig. 2(b) depicts the first and the second TWs reaching the local bus in two consecutive sampling periods, where $1/f_{\mathrm{s}} < t_{\mathrm{F2}} - t_{\mathrm{F1}} < 2/f_{\mathrm{s}}$. Therefore, they would be detected in samples k_{F1} and k_{F1}+1. Nevertheless, this situation would be confused with that one depicted in Fig. 2(a) where k_{F1} and k_{F1}+1 would incorrectly indicate the first and second discrete arriving instants of the TWs. Fig. 2(c) shows a fault exactly in the same position as the fault depicted in Fig. 2(b), i.e., $1/f_{\mathrm{s}} < t_{\mathrm{F2}} - t_{\mathrm{F1}} < 2/f_{\mathrm{s}}$. However, it occurs at a different fault inception time, in a way that the second TW reaches the local bus two sampling periods after the first TW. Therefore, they would be detected in samples k_{F1} and k_{F1}+2. The proposed method defines the uncertainty zone to include the situations shown in Figs. 2(b) and (c), which will be further explained.

The proposed method detects faults when the first and second TWs reach non-consecutive sampling times to overcome the issues addressed in Fig. 2. Therefore, this paper proposes that a DC internal fault is only detected when:

$$k_{\mathrm{F2}} - k_{\mathrm{F1}} \geq 2. \tag{14}$$

Based on (4) and (14), an internal fault is detected when:

$$(t_{\mathrm{F2}} - t_{\mathrm{F1}}) + \epsilon_T \geq 2/f_{\mathrm{s}}, \tag{15}$$

where $-1/f_{\mathrm{s}} < \epsilon_T < 1/f_{\mathrm{s}}$. Therefore, depending on the random value of ϵ_T, DC line faults may be detected as DC internal faults when:

$$t_{\mathrm{F2}} - t_{\mathrm{F1}} > 1/f_{\mathrm{s}}. \tag{16}$$

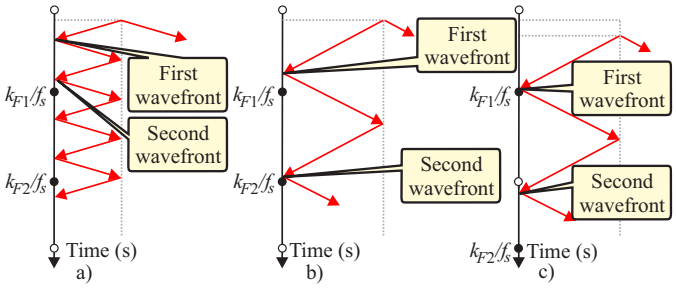

Fig. 2. Faults close to the bus station i: a) t_{F2}-t_{F1}<$1/f_s$; b) $1/f_s$<t_{F2}-t_{F1}<$2/f_s$; c) $1/f_s$<t_{F2}-t_{F1}<$2/f_s$.

Conversely, based on Figs. 2(a) and 2(b), a DC line fault is detected as external DC fault with the time criteria if:

$$k_{F2} - k_{F1} \leq 1. \tag{17}$$

Thus, from (4) and (17) and considering the limits of ϵ_T, DC line faults may be detected as external ones when:

$$t_{F2} - t_{F1} < 2/f_s. \tag{18}$$

Based on (16) and (18), a DC line fault can be detected as either DC internal or external faults with the time criteria if:

$$1/f_s < t_{F2} - t_{F1} < 2/f_s. \tag{19}$$

Thus, the continuous-time boundary of the protected zone is:

$$t_{F2} - t_{F1} = 2/f_s, \tag{20}$$

and the continuous-time boundary of the unprotected zone is:

$$t_{F2} - t_{F1} = 1/f_s. \tag{21}$$

D. The Protected Zone

Besides the discrete-time criterion in (14), this paper also proposes a distance criterion. The distance propagated by TWs in a time equivalent to one sampling time, called in this paper as sampling distance, is given by:

$$\Delta d = v/f_s. \tag{22}$$

According to (20), for a fault on the border of the protected zone, the propagation time from the fault point to the local bus is equal to a sampling time, i.e., $(t_{F2} - t_{F1})/2 = 1/f_s$. Therefore, DC line faults are detected as internal when:

$$\Delta d \leq d_F \leq d - \Delta d, \tag{23}$$

which is the distance criterion for internal DC fault detection. Thus, the length of the protected zone (PZ) is given by:

$$d_{PZ} = d - 2\Delta d = d - 2v/f_s, \tag{24}$$

where $d > 2\Delta d$, i.e., the line length must be higher than $2\Delta d$ to have a protection zone. The number of DC line sampling distance divisions is given by:

$$\Gamma = \lfloor d/\Delta d \rfloor = \lfloor df_s/v \rfloor . \tag{25}$$

and a central portion with a length of $\Delta d1$ given by:

$$\Delta d1 = d - \Gamma\Delta d = d - \lfloor df_s/v \rfloor \, v/f_s. \tag{26}$$

Since the DC line is divided into portions of the sampling distance Δd from each terminal towards the line center and considering (23), the protected zone has Γ-2 sampling distance divisions. Fig. 3 depicts the unprotected (UPZ), uncertainty (UZ), and protected (PZ) zones. The longer the line, the larger the protected zone for a fixed sampling frequency f_s. However, high f_s will result in high protection zones.

E. The Unprotected Zones

According to (21), when a fault takes place in the border of the UPZ, the wavefront takes half of one sampling time to reach the local bus, i.e., $(t_{F2} - t_{F1})/2 = 1/(2f_s)$. Therefore, DC line faults are always detected as DC external faults with the distance criteria when:

$$0 \leq d_F \leq \Delta d/2 \tag{27}$$

or

$$d - \Delta d/2 \leq d_F \leq d. \tag{28}$$

Therefore, the length of the UPZ at each line terminal is:

$$d_{UPZ} = \Delta d/2 = v/2f_s. \tag{29}$$

The UPZ is a blind spot located at each DC line terminal as a consequence of the sampling process. This is important for the TW-based protection security because, although it results in the failure to detect close-in DC line faults, it guarantees that external faults or events, including DC faults in the bus, will never be detected as internal DC line faults.

F. The Uncertainty Zones

According to (19), the UZ is between the boundaries of the PZ and UPZs. Therefore, in terms of distance, a DC line fault may be detected as either DC internal or external faults if:

$$\Delta d/2 < d_F < \Delta d \tag{30}$$

or

$$d - \Delta d < d_F < d - \Delta d/2, \tag{31}$$

where (19) delimits the time limits whereas (30) and (31) delimit the space limits of the local and remote UZ, respectively. From (30) and (31), the length of the UZ at each line terminal is given by:

$$d_{UZ} = \Delta d/2 = v/2f_s. \tag{32}$$

The fault inception time t_F occurs from k_F/f_s to $(k_F+1)/f_s$, according to Fig. 1, whereas the local UZ is delimited in space from $\Delta d/2$ to Δd according to (30). These limits define the time-space region of the local UZ. Fig. 4 depicts the time-space region of the local UZ (Fig. 4(a)) and remote UZ (Fig. 4(b)-(d)), highlighting the borders where faults are detected as internal (yellow regions) or external (orange regions) ones by the proposed method. Faults at the same position inside the UZ may be detected as either internal or external faults because, beyond the fault position, the fault

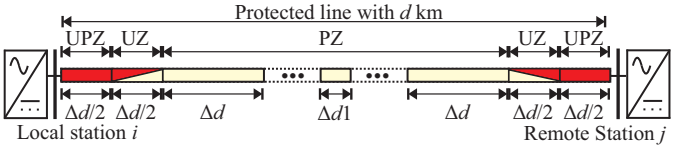

Fig. 3. Uncertainty, unprotected, and protected zones.

inception time also affects this diagnosis. For instance, Faults F1 and F2 in the local UP in Fig. 4(a) with the same position and different fault inception times would be identified as internal and external faults, respectively. The geometry of the time-space region of the UZs, as depicted in Fig. 4, can be mathematically defined by analysing border conditions of the fault inception time t_{F} associated with the ones of the fault distance d_{F}. The shape of the local UZ (Fig. 4(a)) does not change with the line length, whereas the shape of the remote UZ (Fig. 4(b)-(d)) changes with the line length and moves in the time axis in a proportion related to the size $\Delta d1$.

G. Effect of the TW Speed Estimation Accuracy

The real value of the TW propagation speed v is unknown, and its estimation v_T introduces errors to distinguish internal from external faults. Based on (11) and (14) and considering the effect of v_T, internal faults are identified if:

$$2 \leq k_{\mathrm{F2}} - k_{\mathrm{F1}} < \lfloor p df_{\mathrm{s}}/v_T \rfloor , \tag{33}$$

where the term $k_{\mathrm{F2}} - k_{\mathrm{F1}}$ is governed by the unknown TW real propagation speed v. However, $k_{\mathrm{F2}} - k_{\mathrm{F1}}$ is compared to $\lfloor p df_{\mathrm{s}}/v_T \rfloor$, which follows the estimated TW propagation speed v_T. Therefore, the internal fault detection is in accordance with two velocities, i.e., v and v_T, which may lead to trip errors on the borders of the PZ.

Considering the border in (7), i.e., $k_{\mathrm{F2}} - k_{\mathrm{F1}} = \lfloor df_{\mathrm{s}}/v \rfloor + 1$, an internal fault would be detected as an external one if:

$$\lfloor df_{\mathrm{s}}/v \rfloor + 1 \geq \lfloor p df_{\mathrm{s}}/v_T \rfloor , \tag{34}$$

whereas considering the border in (10), i.e., $k_{\mathrm{F2}} - k_{\mathrm{F1}} = \lfloor 2df_{\mathrm{s}}/v \rfloor$, an external fault would be detected as internal if:

$$\lfloor 2df_{\mathrm{s}}/v \rfloor < \lfloor p df_{\mathrm{s}}/v_T \rfloor , \tag{35}$$

which must be always avoided in order to ensure the protection operation security. Considering that the maximum value of p is 2, (35) is always false by adopting $v_{\mathrm{T}} > v$.

Theoretically, the highest value possible for the TW propagation speed is equal to the speed of light (c = 300000 km/s). However, the real speed is always lower than this. Therefore, the way to be totally true that $v_T > v$ is to consider the propagation speed as the speed of light, $v_T = c$. Thus, due to the error in the v_T regarding v, an internal fault may be detected as external one according to (34). However, the protection operation security is ensured according to (35), i.e., external faults would not be detected as internal ones.

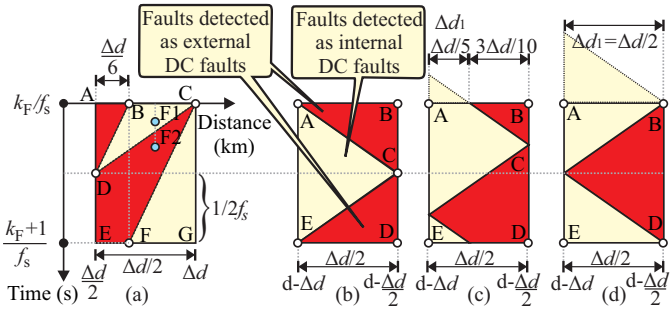

Fig. 4. Boundaries of the uncertainty zones for: a) the local terminal; b) the remote terminal when $\Delta d1$=0 c) the remote terminal when $\Delta d1$=$\Delta d/5$; d) the remote terminal when $\Delta d1$=$\Delta d/2$.

Taking into account that $a - b \geq x$ implies that $\lfloor a \rfloor - \lfloor b \rfloor \geq x$, where $x \in \mathbb{N}$, and considering $v_T = c$, the inequality (34) is false when:

$$p df_{\mathrm{s}}/c - df_{\mathrm{s}}/v \geq 2, \tag{36}$$

which yields:

$$f_{\mathrm{s}} \geq 2c/(d(p - c/v)). \tag{37}$$

That is, the inequality (37) must be respected in order to prevent an internal fault from being detected as an external one when $v_T = c$. This indicates the minimum sampling rate whereby the trip error will not occur.

For given values of d and p, the decrease of v increases $2c/(d(p - c/v))$. In general, the real propagation speed in aerial transmission lines is superior to $0.6c$, as reported in [17], [15]. Therefore, considering these values, it is possible to delimit that the real speed must be in the following range:

$$0.6c \leq v < c. \tag{38}$$

To ensure that no trip error will occur for any real speed based on [17], [15], in (37) v must be replaced by the inferior limit of (38), satisfying, therefore, the minimum sampling frequency established if any speed higher than $0.6c$ was used. Consequently, (37) becomes:

$$f_{\mathrm{s}} \geq 2c/(d(p - 1/0.6)). \tag{39}$$

That is, any sampling frequency higher than or equal to $2c/(d(p-1/0.6))$ ensures that no trip error will occur when the speed is estimated as speed of light ($v_T = c$), since $v \geq 0.6c$. From (39), $1/0.6 < p \leq 2$ for ensuring a positive minimum sampling frequency and respecting (13).

H. The Proposed TW-Based Line Protection

The accurate estimation of the real TW propagation speed v is a recurring problem in the TW methods because it depends on the accurate estimation of transmission line parameters, which can change, for instance, with the local weather. Therefore, this paper suggests using the speed of light c, which makes the method independent of the transmission line parameters and it avoids protection misoperation as well, as addressed in the subsection II-G, since (39) will be respected and $v \geq 0.6c$. In addition, p must be equal to 2 to ensure a smaller minimum sampling frequency established by the inequality (39), avoiding excessive sampling rates. Therefore, according to (33), an internal fault is detected if:

$$2 \leq k_{\mathrm{F2}} - k_{\mathrm{F1}} < \lfloor 2df_{\mathrm{s}}/c \rfloor , \tag{40}$$

and the minimum sampling frequency for the method, according to (39), is given by:

$$f_{\mathrm{s}} \geq 6\,(c/d)\,, \tag{41}$$

where d is the line length in km.

According to (24), (29), and (32), the length of the PZ depends on the real TW propagation speed. However, as $v_{\mathrm{T}} = c$ is adopted, the estimated length of the PZ is smaller than the real one. Conversely, the estimated lengths of the UPZs and UZs are greater than the real ones. This represents a conservative estimation for the zones, which increases the protection dependability.

III. PERFORMANCE EVALUATION

Fig. 5 depicts the simplified topology of the LCC-HVDC transmission system used to assess the performance of the proposed protection system. This is a benchmark model based on an actual bipolar system of ±600 kV and 3150 MW/pole [18]. It was modeled on the EMTP/ATPDraw software and is available for download in [19]. The protected DC transmission line and the external AC transmission lines were replaced in the original ATP model by JMarti frequency-dependent distributed parameter line models. The DC transmission line was modeled according to its geometrical parameters shown in Fig. 6 [20]. The adjacent AC transmission lines are 100 km. Their geometrical parameters are based on an actual 230-kV system and are available in [15].

The validation of the protection inequation given by (40) and the protection zones given by (24), (29), and (32) requires accurate detection of the two first wavefront arrival times. However, the proposal and validation of a TW detection method are outside the scope of this paper and any existing accurate TW detection method can be used. Therefore, this paper considered the TW arrival time detection method proposed by [16]. To ensure no errors in the TW detection method and identify the effects of the sampling frequency in the proposed protection function, faults were simulated with a low resistance to produce a high incidence of electromagnetic transients. Other issues that affect the TW detection method, such as the mixing mode phenomena [21], did not result in errors in the TW detection method.

To evaluate the performance of the proposed method, the following scenarios were simulated: 1) pole-to-ground faults on the DC line and at the local and remote buses with a resistance equal to 1 Ω; 2) three-phase faults in the AC power system with a resistance of 1 Ω.

The theory developed in this paper is true for both voltages and currents because the first and reflected wavefronts can be found in both voltages and currents. However, the voltage signals were used for the evaluation of the results. Measuring instruments were not modeled, i.e., they were considered ideal.

A. Reach of the Zones

Some TW-based line protection algorithms proposed in literature adopts sampling frequencies in the order of hundreds of kHz to minimize the unprotected portion of the transmission line [8], [13]. However, previous works have not demonstrated a clear and precise criterion for definition of the sampling frequency in HVDC power systems.

This paper performs an enhanced mathematical analysis of the sampling frequency effects on the protection zones and demonstrates that the minimum sampling frequency defined in (41) is in the range of a few kHz. This analysis also allowed a precise definition of the sampling frequency as a function of the protection zones. As per (24), if v and d are known, the length of the protected zone at a given sampling frequency can be established; and the length of the protected zone increases with sampling frequency. However, reasonable protected zones can be achieved with a sampling frequency on the order of tens of kHz. For instance, for a 2900 km transmission line, the protected zone is 97% with a sampling frequency of 10 kHz, and that will increase to 99% for 25 kHz. On the other hand, according to (29), a very small d_{UPZ} of approximately 1 km requires a sampling frequency of 150 kHz.

B. Assessment of the Theoretical Protection Zones

The proposed method does not require TW propagation speed estimation. As mentioned before, in real-world systems, the protection zones can be conservatively estimated by using $v_T = c$. The validation of the exact theoretical protection zones can be accomplished considering the exact TW propagation speed, in a fixed low sampling frequency and varying the line length.

For the assessment of the theoretical protection zones, faults were applied along the protected transmission line. The adopted relay sampling frequency was 10 kHz and the simulation step-size was a hundred times lower than the sampling period, i.e., 1 μs. For the validation of the UZs and UPZs, the TW propagation speed estimation was performed through a practical procedure performed in actual power systems [17]. In an actual system, the DC line can be energized from the local station. In this procedure, the AC breaker in the local station is closed while the AC breaker in the remote station remains open. As soon as the transistors are fired, the time stamps of voltages and currents can be measured at the local station after the DC reactor, on the transmission line. Afterward, the wave is transmitted along the transmission line toward the remote station and reflected back to the local station. Therefore, the time stamp of the reflected wave from the remote station can be measured.

Considering the protected transmission line of 2900 km in length, the TW propagation speed was estimated as v = 297.4359 km/ms (0.9915c). Considering the estimated TW propagation speed and the adopted sampling frequency, according to (29) and (32), the length of the UZ and UPZ at each line terminal are 14.87 km.

For the validation of the UZs and UPZs, 11 faults were applied at each fault point, considering fault inception times from 0 to 100 μs, at steps of 10 μs. This enabled the evaluation of the effect of the fault inception time on these zones. Taking into account that the shape of the local UZ does not change with the length of the protected line, three cases of protected line lengths and corresponding fault locations were considered: 1) a 2900 km transmission line: faults were simulated in the ranges of 1 km to 31 km and 2869 km to 2899 km at 1 km intervals, resulting in 682 faults; 2) a 2885.1282 km

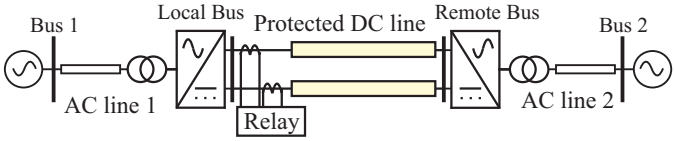

Fig. 5. Test power electrical system.

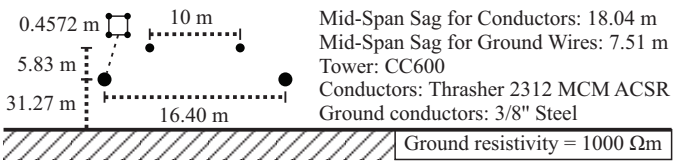

Fig. 6. Geometrical parameters of the DC transmission line.

long transmission line: fault were applied in the range from 2855.1282 to 2781.1282 km at intervals of 1 km, in a total of 187 faults; 3) a 2891.0769 km long transmission line: faults were applied in the range from 2877.0769 km to 2891.0769 km at intervals of 1 km, resulting in a total of 187 faults.

These specific line lengths were adopted in order to evaluate the UZs and UPZs for $\Delta d1 = \Delta d/2$, $\Delta d1 = 0$, and $\Delta d1 = \Delta d/5$, which represents, respectively, d = 2900 km, d = 2885.1282 km, and d = 2891.0769 km, where Δd and $\Delta d1$ are defined in (22) and (26), respectively.

Fig. 7 depicts the theoretical UZs and UPZs of the protected line, which consists of a unique local UZ and three remote UZs according to the selected line lengths. The circles represent the simulated faults detected either as internal or external faults. These results refer to an estimated TW propagation speed, whereby its exact value is unknown. Transmission lines modeled with frequency-dependent parameters are closer to reality and impose variation on the wave velocity according to the fault location. The longer the distance the wave travels, the lower the velocity estimated. Therefore, wave velocity estimation always presents errors. Thus, uncertainties are expected at the boundary of the theoretical fault detection regions. Almost all faults were detected within their related theoretical fault detection region. Therefore, even considering uncertainties in estimating the TW propagation speed, the lengths and shapes of the protection zones can be mathematically predicted with high accuracy.

In real-world systems, c can be used as the TW propagation speed in the protection inequality (40) and for the protection zone estimations in (32), (29), and (24). Therefore, as discussed in previous sections, the method proposed does not require wave speed estimation. Thus, for the fault scenarios depicted in Fig. 7 and considering the TW propagation speed equal to c, the length of the UZs and UPZs are conservatively re-estimated to be 15 km long. Simulation results show that for all 1056 fault cases evaluated, only one fault within the UPZ was detected as internal. As depicted in Fig. 7(a), this fault case was at the boundary of the local UPZ. As the length of the UZs and UPs increases, the chance for an external fault to be detected within the PZ decreases. Indeed, all the faults detected as external were within the UZs or UPZs. Thus, the conservative estimation of the protection zones increased the protection security and allowed the non-requirement of TW propagation speed estimation, which is a source of errors.

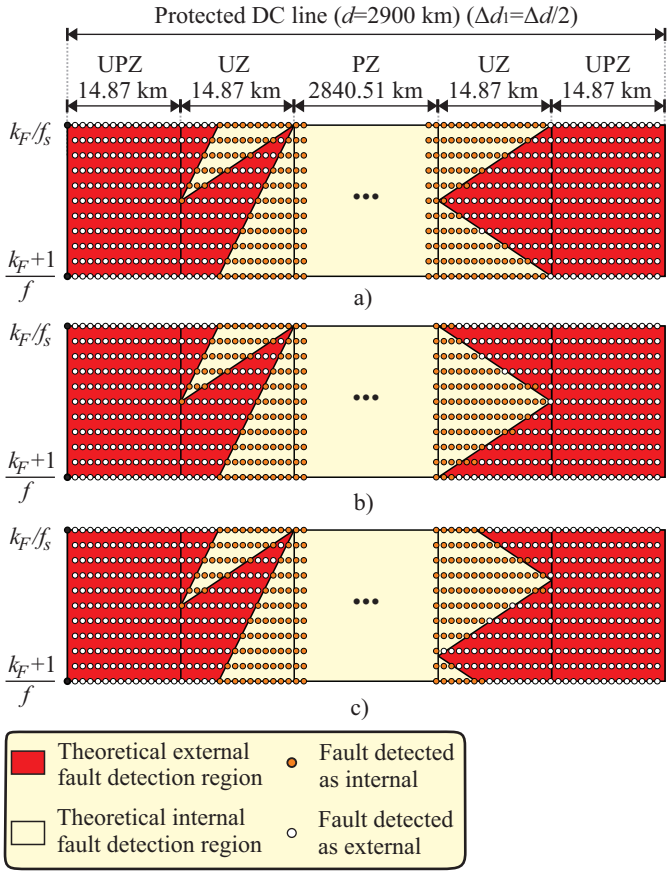

Fig. 7. Protection zones for: a) d = 2900 km; b) d = 2885.13 km ($\Delta d_1 = 0$); c) d = 2891.08 km ($\Delta d_1 = \Delta d/5$).

For the evaluation of the protection operation time for faults applied in the PZ, faults were applied from 50 to 2850 km, at steps of 50 km, considering a protected line of length 2900 km. The TW propagation speed equal to c was considered. Fig. 8 depicts the protection operation time as a function of the fault location. All applied faults were detected as internal ones according to (40), demonstrating the existence of the PZ, as expected. The relay operation time of the proposed method is a function of the arrival time of second wave front, $(k_{F2}/f_s) - t_F$. The maximum operation time was lower than 15 ms.

C. External Faults

External faults were also simulated to verify the security of the proposed method. Therefore, faults were applied on both local and remote DC buses as well as on both AC systems. Specifically, faults on the DC buses were applied immediately behind the DC reactor, on the converter side. Faults on both local and remote DC buses were successfully detected as DC external faults, according to (40). AC faults were simulated on the AC transmission lines at 20, 40, 60, and 80 km from the converters as well as on both sides of the converter transformers. As expected, the AC system faults did not generate TWs on the local DC bus. This is because the filters on both AC and DC sides of the converters block the propagation of TWs from the AC side to the DC measurement point. Therefore, AC faults were not detected as internal faults.

D. Qualitative Comparison with other TW Functions

This paper proposes improvements in the classical one-terminal traveling wave (1T)-based protection by including the sampling frequency effects of digital signals, resulting in protection zones. [13] presented improvements in a classical two-terminal traveling wave (2T)-based

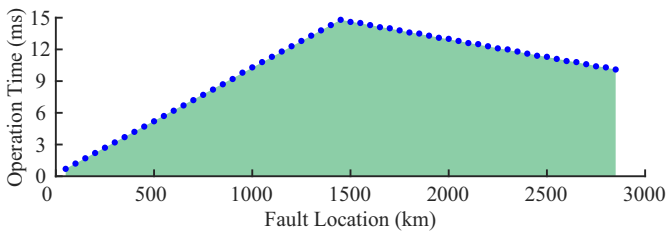

Fig. 8. Operation time for the proposed protection.

protection considering protection zones. Therefore, 1T and 2T are classical traveling wave protections. Other widespread traveling wave functions using other concepts are TW32, based on directional elements, and TW87, based on differential elements.

The 2T, TW32, and TW87 detect the first incident TWs that reach the monitored buses, whereas 1T requires the first and reflected TWs. Thus, 2T, TW32, and TW87 depend on a communication system, whereas 1T does not need one. Conversely, 2T, TW32, and TW87 require the simplest digital signal processing tools to detect only the first incident TW. Close-in faults are issues to 1T and 2T TW functions. However, by including the effects of the sampling frequency, they present well-defined protected and unprotected zones with small unprotected zones for a typical sampling frequency of 1 MHz. Based on directional principles, the TW32 can distinguish forward from reverse faults, whereas based on differential principles, the TW87 distinguishes internal from external faults. Therefore, close-in faults are not issues for TW32 and TW87. Nevertheless, TW32 and TW87 require both voltage and current signals, whereas 1T and 2T can adequately work with only currents, if necessary, to become unaffected by voltage measurement issues. Furthermore, time synchronization is not an issue for the TW32 because it needs only relative polarities, whereas time synchronization affects TW87 and 2T functions. The functions 1T, 2T, TW32, and TW87 are based on widespread TW monitoring technology, and coordinating all these functions would result in the fastest and most accurate TW-based protection.

IV. Conclusion

This paper proposes a one-terminal TW-based protection applied to LCC-HVDC transmission lines. The method requires the first two wavefronts to reach the local bus. Thus, a communication system is not required. Due to the boundary conditions of LCC-HVDC systems, the method is not sensitized by faults on external transmission lines.

A thorough mathematical investigation of the sampling frequency effects on the protection was performed so that some known limitations associated with TW-based methods were successfully addressed. The method does not require a TW propagation speed estimation for transmission lines with TW propagation speed lower than $0.6c$. Instead, the speed of light can be adopted without loss of dependability. Protected, unprotected, and uncertainty zones can be mathematically estimated. Thereby, the method is able to distinguish between faults on the line terminals and faults on the protected transmission line. An inequality for the minimum sampling frequency required for trustworthy protection was developed. For a fixed sampling frequency, the shorter the transmission line, the shorter the protection zone. Thereby, the method revealed a reliable performance considering a sampling frequency equal to 10 kHz on a line of 2900 km in length. The proposed protection presented operation time below 15 ms, without loss of dependability.

The proposed protection zones can be extended to point-to-point HVDC with voltage-source converter (VSC) technology. However, further development is required for multi-terminal VSC-HVDC systems. Additionally, further development is required for the method to be applied to underground cables. Limitations in the traveling wave detection method will affect the proposed method. Thus, the effects of fault resistance and other parameters such as the mixing mode phenomena must be verified in further work.

References

[1] J. Wu, H. Li, G. Wang, and Y. Liang, "An Improved Traveling-Wave Protection Scheme for LCC-HVDC Transmission Lines," *IEEE T Power Deliver*, vol. 32, no. 1, pp. 106–116, 2017.

[2] B. Li, Y. Li, J. He, B. Li, S. Liu, B. Liu, and L. Xu, "An improved transient traveling-wave based direction criterion for multi-terminal hvdc grid," *IEEE T Power Deliver*, 2020.

[3] D. Tzelepis, A. Dyśko, G. Fusiek, J. Nelson, P. Niewczas, D. Vozikis, P. Orr, N. Gordon, and C. D. Booth, "Single-ended differential protection in mtdc networks using optical sensors," *IEEE T Power Deliver*, vol. 32, no. 3, pp. 1605–1615, 2017.

[4] X. Zheng, T. Nengling, Y. Guangliang, and D. Haoyin, "A transient protection scheme for hvdc transmission line," *IEEE T Power Deliver*, vol. 27, no. 2, pp. 718–724, 2012.

[5] J. Liu, N. Tai, and C. Fan, "Transient-voltage-based protection scheme for dc line faults in the multiterminal vsc-hvdc system," *IEEE T Power Deliver*, vol. 32, no. 3, pp. 1483–1494, 2017.

[6] Z. Zheng, T. Tai, J. S. Thorp, and Y. Yang, "A transient harmonic current protection scheme for hvdc transmission line," *IEEE T Power Deliver*, vol. 27, no. 4, pp. 2278–2285, 2012.

[7] G. Song, X. Chu, S. Gao, X. Kang, and Z. Jiao, "A new whole-line quick-action protection principle for hvdc transmission lines using one-end current," *IEEE T Power Deliver*, vol. 30, no. 2, 2015.

[8] X. Liu, A. H. Osman, and O. P. Malik, "Hybrid traveling wave/boundary protection for monopolar hvdc line," *IEEE T Power Deliver*, vol. 24, no. 2, pp. 569–578, 2009.

[9] Y. Zhang, N. Tai, and B. Xu, "Fault analysis and traveling-wave protection scheme for bipolar hvdc lines," *IEEE T Power Deliver*, vol. 27, no. 3, pp. 1583–1591, 2012.

[10] F. Kong, Z. Hao, S. Zhang, and B. Zhang, "Development of a novel protection device for bipolar hvdc transmission lines," *IEEE T Power Deliver*, vol. 29, no. 5, pp. 2270–2278, 2014.

[11] F. Kong, Z. Hao, and B. Zhang, "A novel traveling-wave-based main protection scheme for $\pm$800 kv uhvdc bipolar transmission lines," *IEEE T Power Deliver*, vol. 31, no. 5, pp. 2159–2168, 2016.

[12] E. O. Schweitzer, B. Kasztenny, and M. V. Mynam, "Performance of time-domain line protection elements on real-world faults," in *2016 69th Annual Conference for Protective Relay Engineers (CPRE)*, 2016.

[13] F. B. Costa, A. Monti, F. V. Lopes, K. M. Silva, P. Jamborsalamati, and A. Sadu, "Two-terminal traveling-wave-based transmission-line protection," *IEEE T Power Deliver*, vol. 32, no. 3, p. 1382–1393, 2017.

[14] F. B. Costa, F. V. Lopes, K. M. Silva, K. M. C. Dantas, R. L. S. França, M. M. Leal, and R. L. A. Ribeiro, "Mathematical development of the sampling frequency effects for improving the two-terminal traveling wave-based fault location," *Int J Elec Power*, 2020.

[15] R. L. S. França, F. C. Silva Júnior, T. R. Honorato, J. P. G. Ribeiro, F. B. Costa, F. V. Lopes, and K. Strunz, "Traveling wave-based transmission line earth fault distance protection," *IEEE T Power Deliver*, vol. 36, no. 2, pp. 544–553, 2021.

[16] D. M. Silva, F. B. Costa, V. Miranda, and H. Leite, "Wavelet-based analysis and detection of traveling waves due to dc faults in lcc hvdc systems," *Int J Elec Power*, vol. 104, no. 1, pp. 291–300, 2019.

[17] E. O. Schweitzer, A. Guzmán, M. V. Mynam, V. Skendzic, B. Z. Kasztenny, and S. Marx, "Protective relays with traveling wave technology revolutionize fault locating," *IEEE Power Energy M*, vol. 14, no. 2, pp. 114–120, 2016.

[18] N. F. d. S. G. S. Luz, "First benchmack model for hvdc controls in atp program," in *X Symposium of specialists in electric operational and expansion planning, Florianópolis (SC), Brazil*, 2006.

[19] G. S. Luz. (2016) R2-mad-new4d. (Accessed: 2021-03-23). [Online]. Available: https://www.atpdraw.net/showpost.php?id=52&kind=0

[20] G. S. Luz, D. S. C. Junior, and S. G. Junior, "Hvdc transmission line modeling analysis in pscad and atp programs," in *XIII Symposium of Specialists in Electric Operational and Expansion Planning*, 2014.

[21] F. M. de Magalhães Júnior and F. V. Lopes, "Mathematical study on traveling waves phenomena on three phase transmission lines – part ii: Reflection and refraction matrices," *IEEE T Power Deliver*, vol. 37, no. 2, pp. 1161–1170, 2022.